JCTC Journal of Chemical Theory and Computation

Article

pubs.acs.org/JCTC

Interaction of Nucleic Acid Bases with the Au(111) Surface

Marta Rosa,[†,‡] Stefano Corni,[†] and Rosa Di Felice*[,†]

[†]Center S3, CNR Institute of Nanoscience, Via Campi 213/A, 41125 Modena, Italy

[‡]Department of Physics, University of Modena and Reggio Emilia, 41125 Modena, Italy

Supporting Information

ABSTRACT: The fate of an individual DNA molecule when it is deposited on a hard inorganic surface in a "dry" environment is unknown, while it is a crucial determinant for nanotechnology applications of nucleic acids. In the absence of experimental approaches that are able to unravel the three-dimensional atomic structure of the target system, here we tackle the first step toward a computational solution of the problem. By using first-principles quantum mechanical calculations of the four nucleobases on the Au(111) surface, we present results for the geometries, energetics, and electronic structure, in view of developing a force field that will enable classical simulations of DNA on Au(111) to investigate the structural modifications of the duplex in these non-native conditions. We fully characterize each system at the individual level. We find that van der Waals interactions are crucial for a correct description of the geometry and energetics. However, the mechanism of adsorption is well beyond pure dispersion interactions. Indeed, we find charge sharing between the substrate and the adsorbate, the formation of hybrid orbitals, and even bonding orbitals. Yet, this molecule−surface association is qualitatively distinct from the thiol adsorption mechanism: we discuss such differences and also the relation to the adsorption mechanism of pure aromatic molecules.

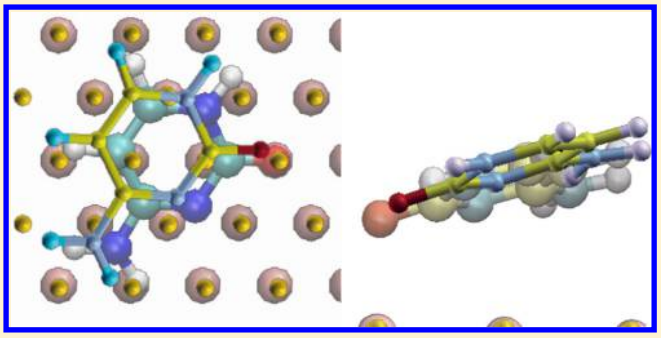

1. INTRODUCTION

DNA, the molecule of life, has been a fascinating research subject since its discovery.[1,2] The determination of its three-dimensional structure in 1953[3] boosted investigations to understand the miriad of biological and medical phenomena in which it is involved, such as DNA−protein interactions for genetic transcription and replication, the evolution of the species, cancer development and treatment, genetic diseases due to mutations and many others. Research on nucleic acids has always been inherently interdisciplinary, encompassing biology, chemistry, and medicine.

In recent years, new applications of DNA are envisaged, which require the usage of physics and nanotechnology tools. In fact, given its intrinsic task of storing and translating information, scientists have started to ask the question whether its physico−chemical nature makes it able to store and transfer charges as well. Concepts and achievements in this direction are summarized in recent reviews.[4−7] Several new techniques (e.g., DNA chips) and applications (e.g., molecular electronics) require the interaction of DNA molecules with nonliving entities, such as inorganic substrates and fluorophores. The interaction of DNA molecules with inorganic surfaces is particularly puzzling, because the "hard" environment, so different from the natural solution environment of the cells, may induce denaturation and unfolding. To mention only a couple of general examples: DNA molecules are deposited "horizontally" on metal or insulating substrates for scanning tunneling microscopy/spectroscopy (STM/STS)[8−10] and atomic force microscopy (AFM)[4,11,12] investigations of the morphology and electronic structure; thiol-functionalized DNA molecules are attached "perpendicularly" to metal electrodes to measure the charge transport capabilities.[13−16] The height of double-stranded DNA molecules deposited "horizontally" on a hard substrate, measured by AFM, is about 50% of the diameter in solution,[11,12] which suggests possible unfolding of the nucleic acid in such experimental conditions. However, no confirmation of this hypothesis exists. Knowledge of the structure of DNA molecules on a hard substrate is extremely important to determine their ability to conduct charges in setups relevant for nanotechnologies, because the electronic structure and transfer rates are extremely sensitive to the conformational details.[17−20] This knowledge is not accessible through conventional methods for the determination of the three-dimensional atomic structure of biological molecules, such as X-ray or NMR, which are not compatible with the substrate environment. Therefore, we have undertaken a long-term plan to investigate this problem by computational means.

Classical molecular dynamics (MD) atomistic simulations are in principle a method of choice. They have successfully been employed to describe the unfolding of biological molecules in solution.[21−23] However, the crucial point in any classical MD methodology is the parametric force field (FF), which is the potential energy necessary for the evolution of the atomic

Received: March 26, 2013
Published: August 27, 2013

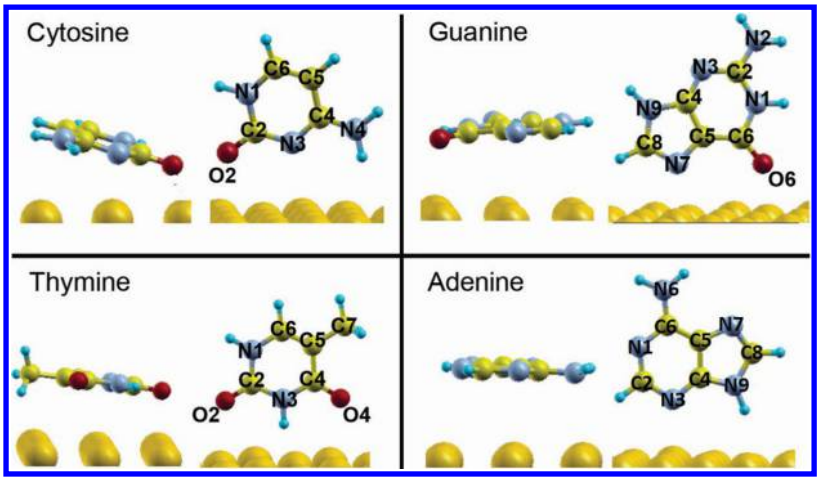

Figure 1. Optimized vdW−DF three-dimensional structures for the most favorable horizontal (left part in each panel) and vertical (right in each panel) adsorption configurations among those considered by us for cytosine (C), guanine (G), thymine (T), and adenine(A) on Au(111). Only the top atomic plane of the substrate is shown (large golden spheres). Small yellow, cyan, red, and turquoise spheres represent C, N, O, and H atoms of the molecule.

coordinates in time according to Newton's equations.[24,25] Reliable force fields exist for liquid, solid, and molecular materials, but the description of the interaction between molecules and hard inorganic surfaces is still in its infancy. Our group has developed force fields for the interaction of proteins with the Au(111) surface,[26,27] and we have recently reviewed our computational approach in this context, as well as similar efforts by other groups.[28] We now plan to extend this approach to the interaction of nucleic acids with the Au(111) surface, which requires specific parametrization due to different functional groups and heterocycles of the bases. As described elsewhere,[28] the first step of a viable multistep methodology is the derivation of a classical force field by means of density functional theory (DFT) calculations of small molecules on the target surface. The outcome of this approach sheds light not only on the energetics that is the basis of the force field but also on the adsorption mechanisms and charge redistribution.[29] This article pursues this objective for the adsorption of DNA bases on the Au(111) surface. Our research connects to a variety of lively investigations for the development of DNA microarray techniques,[30] portable cost-effective DNA sequencing,[31] targeted drug delivery,[32] formation of self-assembled superstructures,[33−35] and the development of life under prebiotic conditions.[36] It is also related to recent studies to assess atomistic computational methods for unraveling crucial features linked to the geometry and to the electronic structure.[33,35,37−39]

We have already described the "horizontal" adsorption of cytosine on Au(111) by DFT as a model system to prove the crucial role of van der Waals (vdW) interactions in the description of DNA bases on surfaces.[40] We have shown that several configurations are quasi-isoenergetic and need to be considered for the derivation of a new classical FF. The four bases cytosine, guanine, thymine, and adenine need to be studied one by one on the same footing, because experimental data show that they behave in a very different way on Au(111).[41−47] Guanine and adenine self-assemble in monolayer structures.[43] Cytosine forms filaments rather than self-assembled monolayers.[45−47] Thymine behaves in an intermediate way, choosing filament or monolayer configurations depending on the molecular density on the surface.[44]

We find that the inclusion of vdW interactions affects differently the adsorption of the four bases, modifying more the internal geometries and adsorption configurations of cytosine and guanine than those of thymine and adenine. We reveal significant differences in the adsorption energies computed with and without vdW terms, which is particularly relevant in view of developing a force field. Our results on the adsorption energies of cytosine (C), guanine (G), thymine (T), and adenine (A) on Au(111) give adsorption strengths in the order $T < C \sim A < G$, which is in line with the outcome of desorption experiments, $T < C \leq A < G$:[48] this is a remarkable success of the vdW dscription, which could not be achieved with gradient-corrected (GGA) or hybrid DFT functionals. Furthermore, our results show that "horizontal" adsorption geometries are favorable with respect to "vertical" orientations for each of the four bases: this has implications for the abilities of monolayer formation. The outcome of our investigation points to an adsorption mechanism that entails adsorbate−substrate electronic mixing and thus cannot be ascribed to solely dispersion interactions.

2. METHOD

We performed gradient corrected DFT calculations of the four DNA bases adsorbed at the Au(111) surface (Figure 1) with the quantum−espresso package version 5.0,[49] using the PBE exchange correlation functional[50] and the vdW−DF functional.[51] The surface was modeled with a slab of four Au layers with a periodically repeated $6 \times 3\sqrt{3}$ surface supercell, with 36 atoms per layer. The lateral size of the supercell was 17.58 × 15.22 Å^2 and 18.00 × 15.59 Å^2 in PBE and vdW−DF calculations of the base/Au(111) interfaces, respectively, obtained from the corresponding bulk fcc Au equilibrium lattice parameter (4.14 Å and 4.24 Å, respectively).

The adsorbate−adsorbate lateral distance between two neighboring replicas was at least 10 Å and the vacuum thickness in the direction perpendicular to the surface was at least 11 Å. Tests in a larger supercell were performed, to check that the chosen size assures no interaction between the molecule and its periodic images. We chose a plane wave basis set with a cutoff of 25 Ry,[29] and we described the electron−ion interaction with ultrasoft pseudopotentials.[52] The valence shells were 2*s* and 2*p* for C, N, and O; 5*d* and 6*s* for Au with a scalar relativistic treatment that was assessed on surface chemistry and

dx.doi.org/10.1021/ct4002416 | J. Chem. Theory Comput. 2013, 9, 4552−4561

Table 1. Calculated Adsorption Energies, Molecule−Surface Distances and Orientations: The Quantities without (with) PBE Superscript Result from vdW−DF (PBE) Calculations[a]

structure[b]	α[c] (deg)	d[d] (Å)	$d^{PBE,c}$ (Å)	E_{ads} (kcal/mol)	E_{ads}^{PBE} (kcal/mol)
		Horizontal Configurations			
${}_h$G@Au(111)^t	83.0	3.0		**23.3**	
${}_h$G@Au(111)^f	87.0	3.2		23.1	
${}_h$G@Au(111)^b	86.0	3.2	3.3	23.0	5.9
${}_h$A@Au(111)^b	87.0	3.2		**19.7**	
${}_h$A@Au(111)^t	87.0	3.2	3.3	19.4	3.9
${}_h$C@Au(111)^t	76.0	2.7		**19.7**	
${}_h$C@Au(111)^b	86.0	3.1	3.4	18.2	4.5
${}_h$C@Au(111)^f	81.0	3.1		18.0	
${}_h$T@Au(111)$^{t+f}$	84.5	3.2÷3.6	3.3÷4.0	**17.2**	2.7
${}_h$T@Au(111)^f	85.6	3.2÷		17.1	
${}_h$T@Au(111)$^{f+t}$	90.0	3.4÷3.4		17.1	
${}_h$T@Au(111)$^{t+t}$	84.1	3.2÷3.4		17.0	
${}_h$T@Au(111)$^{b+f}$	86.6	3.4÷3.6		16.9	
		Vertical Configurations			
${}_v$G@Au(111)$^{t+N7t}$	0.0	2.6	2.9	18.6	10.9
${}_v$G@Au(111)$^{b+N7t}$	0.0	2.6		18.1	
${}_v$G@Au(111)$^{b+N2t}$	41.0	3.0	3.1	16.6	7.9
${}_v$G@Au(111)$^{f+N2t}$	41.0	3.0		16.5	
${}_v$G@Au(111)^{N3t}	30.0	3.3		15.2	
${}_v$A@Au(111)^{N3t}	0.0	2.7	2.5	17.4	10.9
${}_v$A@Au(111)^{N1t}	0.0	2.8		14.4	
${}_v$C@Au(111)$^{t+N3t}$	32.0	2.6	2.2	19.2	15.5
${}_v$C@Au(111)^t	22.0	2.5		12.2	
${}_v$C@Au(111)^f	0.0	2.4		10.9	
${}_v$C@Au(111)^b	0.0	2.3		10.0	
${}_v$T@Au(111)$^{t+b}$	0.0	3.1÷3.3	3.4÷3.5	11.0	2.6
${}_v$T@Au(111)$^{f+b}$	0.0	3.2÷3.2		11.0	
${}_v$T@Au(111)^{O4t}	0.0	2.8		10.1	
${}_v$T@Au(111)^{O2t}	0.0	2.8		7.5	

[a]Bold font marks the lowest-energy vdW−DF structures for C, G, T, and A on Au(111). [b]Labeling conventions are explained in the text. [c]α is the inclination angle of the molecule relative to the vertical axis, from vdW−DF calculations. [d]d is the molecule−surface distance, evaluated for horizontal (vertical) configurations as the distance between the most reactive (nearest) molecular center and the Au atom below it in the outermost substrate plane.

nanostructure formation.[53,54] The Brillouin zone (BZ) sums were calculated including 2 Monkhorst−Pack special **k** points in the irreducible wedge. All the atomic coordinates were relaxed until each force vanished within 0.05 eV/Å. The technical details (basis set, Brillouin zone sums, pseudopotentials) were extensively validated elsewhere for cytosine/Au(111),[40] and based on the similarity of all the computed interfaces, we are confident that they are extendable with the same accuracy to all the systems in this work. The thickness of the Au slab is appropriate for describing interface effects in such extended structures.[55,56]

For comparing different levels of theoretical description, we first relaxed the system at each level until the forces vanished within 0.05 eV/Å and then performed single-point electronic structure calculations at the same level keeping the system coordinates frozen and varying only the distance between the surface and the molecule.

In the following, we denote with the term "formation energy" the difference between the total energy of the interface and the total energies of the isolated constituents. We use the term "adsorption energy" for the opposite of the formation energy: thus, the adsorption energy is negative when the formation of the interface is endothermic, it is positive when the formation of the interface is exothermic.

The lack of dispersion interactions is a well-known shortcoming of standard exchange−correlation functionals in DFT, and this is undoubtedly a major issue in organic materials, molecules, and molecules on inorganic surfaces. Despite the importance of vdW interactions, many studies were done so far for molecules on surfaces by DFT with standard GGA functionals. In this work, we have adopted an up-to-date approach that self-consistently includes vdW terms in electronic structure calculations.[40] Specifically, among recently proposed functionals to treat van der Waals effects within DFT calculations,[51,57−59] we have used the vdW−DF functional.[51] The use of this functional is becoming increasingly benchmarked and accepted for the accurate DFT description of interfaces between organic layers and metal substrates.[60−65] The method was assessed by us on the model system cytosine@Au(111), and here, we exploit the outcome of those tests.[40] In this work, we apply the same approach to the whole set of DNA bases adsorbed on Au(111) in both "horizontal" and "vertical" orientations relative to the substrate.

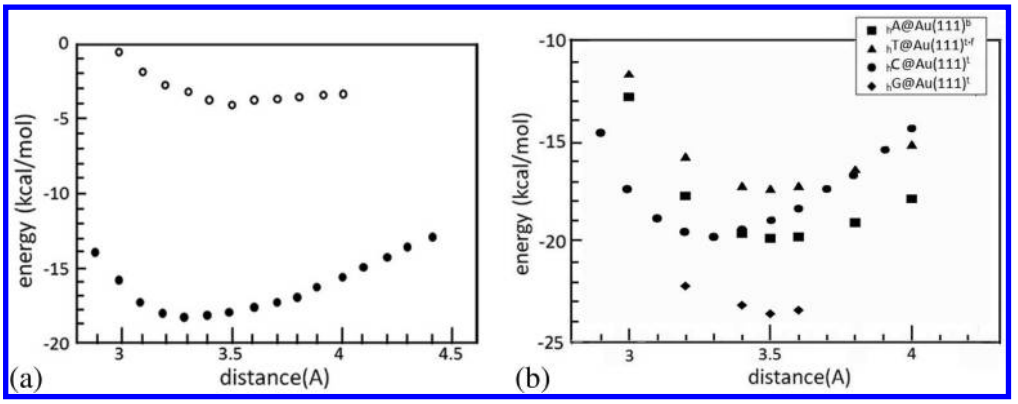

Figure 2. Formation energy versus molecule−Au vertical distance. The vertical distance is measured between the center of mass of the molecule and the average surface height. (a) PBE (circles) and vdW−DF (dots) results for $_h$C@Au(111)^b. The vdW−DF results are in much better agreement than the PBE ones with experimental data.[33,48] Half of the adsorption energy is due to long−range dispersive interactions between the molecules and the surface. (b) vdW−DF results for the four bases in lowest−energy horizontal configurations, as in the legend.

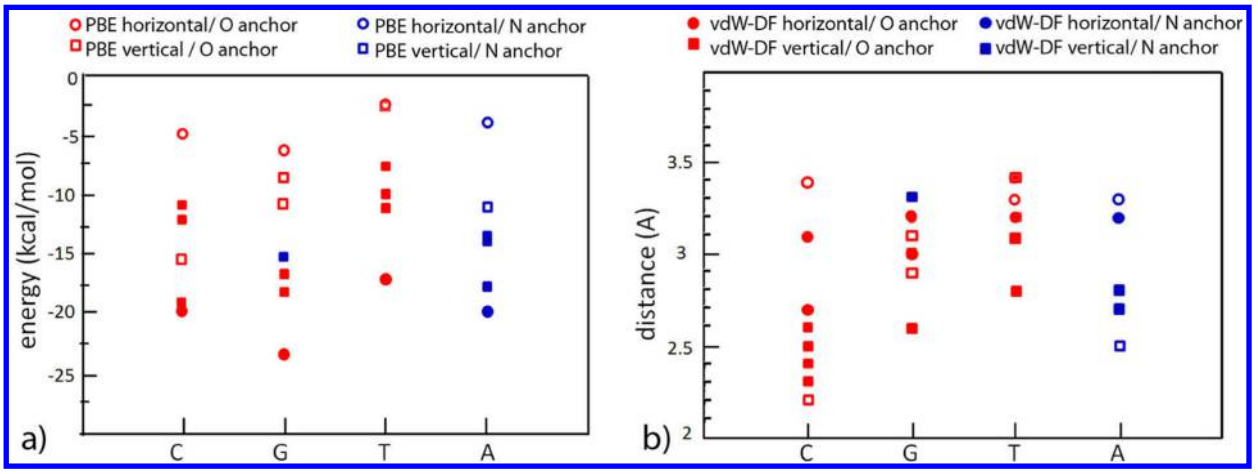

Figure 3. Formation energies in kcal/mol (a) and molecule−surface distances in Å (b) from vdW−DF calculations, for all the structures that we have considered, according to the values in Table 1. Multiple symbols (dots, circles, full squares, open squares) for a certain base report the multiple data from Table 1: accordingly, there are four full squares and three dots for C and similarly for the other bases. Red (blue) symbols represent geometries where an O (N) atom of the molecule is the closest to the surface.

3. RESULTS AND DISCUSSION

3.1. Energetics and Relaxed Geometries. Different adsorption sites (top, bridge, fcc) and adsorption geometries (horizontal and vertical) were sampled for each of the four DNA bases (see Figure S1, Supporting Information). The most favorable geometries are illustrated in Figure 1, which also defines the atom labeling that is used throughout the article.

We considered 13 horizontal configurations, obtained by placing the most reactive atomic center (an atom or a group of atoms) of each base on the three possible sites of the Au(111) triangular lattice. The most reactive atomic center is O2 and O6 for cytosine and guanine, respectively: three horizontal configurations were sampled for each of these two bases. We will label them in the following $_h$C@Au(111)^t, $_h$C@Au(111)^b, $_h$C@Au(111)^f, $_h$G@Au(111)^t, $_h$G@Au(111)^b, $_h$G@Au(111)^f, where the right superscript indicates the adsorption site for the O atom (*t* for top, *b* for bridge, *f* for fcc) and the left subscript *h* indicates a horizontal configuration (later we use the left subscript *v* for vertical configurations). Thymine has two most reactive atomic centers, O2 and O4: we considered five horizontal geometries $_h$T@Au(111) to allow for simultaneous reaction of these two centers. The labels used for the horizontal $_h$T@Au(111) structures are $_h$T@Au(111)$^{t+f}$, $_h$T@Au(111)$^{f+t}$, $_h$T@Au(111)$^{t+t}$, $_h$T@Au(111)^f, $_h$T@Au(111)$^{b+f}$, where the right superscript *t*+*t* (*t* + *f*, *f* + *t*, *b* + *f*) indicates that O2 and O4 are above equivalent top (inequivalent top and fcc, fcc and top, bridge and fcc) sites, while the right superscript *f* indicates that O2 only is above an fcc site of the Au(111) substrate. The most reactive center of adenine is N3; considering hindrance constraints, we identified only two horizontal configurations, $_h$A@Au(111)^b and $_h$A@Au(111)^t, namely with the N3 atom above a bridge and top position. For the vertical configurations, we considered more possibilities, because different inclinations are possible so that more than one atomic centers of the adsorbate reacts with the Au(111) substrate (see Figure S1, Supporting Information, and Table 1). The labels adopted for vertical configurations follow similar criteria as those of horizontal configurations, namely, (1) the superscript *t*, *b*, or *f* indicates that the most reactive atom center (O2 in C, O6 in G, and N3 in A) is above a top, bridge or fcc position of the Au(111) lattice; (2) thymine has two equally reactive atoms, O2 and O4, so we distinguish two vertical configurations in which one O atom is binding to gold (superscripts O2t and O4t); (3) to denote structures in which multiple molecular centers are close to the substrate we use the symbol +, and we explicitly indicate which atom is at which position.

dx.doi.org/10.1021/ct4002416 | J. Chem. Theory Comput. 2013, 9, 4552−4561

For each system, we fixed an initial geometry with the molecule at a certain distance from the surface and relaxed all the atomic coordinates. The molecule was exactly parallel (90-degrees tilt angle) and perpendicular (0-degrees tilt angle) to the surface in the initial conditions for the horizontal and vertical configurations, respectively. The initial molecule−surface distance, as measured from the most reactive (closest) atom of the adsorbate to the Au(111) lattice site below it for the horizontal (vertical) molecular orientations, was 3.3 Å (2.8 Å). These values were chosen on the basis of our recent results for C@Au(111).[40] The internal geometry of the adsorbate in all the initial conditions was flat: this implies that for horizontal configurations the starting adsorbate−substrate distance coincides with the distance between the plane of the molecule and the surface.

To verify that the system is not trapped in an irrelevant local minimum by the geometry optimization algorithm, for some configurations, we did a series of single-point calculations at frozen internal coordinates, starting from the optimized structure and varying only the molecule−surface vertical distance over a broad range of distances. The results of this procedure are illustrated for exemplifying cases in Figure 2. In Figure 2a, for the system ${}_{\mu}\mathrm{C@Au(111)}^{b}$, we show the relative performance of the vdW−DF and PBE functionals in the self-consistent calculations. The minima of the curves in Figure 2a give the equilibrium distance and formation energy. Note that PBE calculations yield a very shallow minimum at 3.5 Å, while vdW−DF calculations produce a deeper minimum at a distance between the center of the molecule and the surface of 3.3 Å, which is more compliant with a variety of results on aromatic systems and heterocycles.[66,67] Similar trends as those in Figure 2a are found for all the bases, which means that long-range interactions are fundamental for the correct description of the adsorption of DNA bases on surfaces. In Figure 2b, we visualize the relative behavior of the different bases: this plot identifies the order of adsorption strengths between the various structures. The same concepts are visualized in a different manner in Figure 3.

The analysis of Figures 2 and 3, along with Table 1 and the consideration of all the equilibrium structures, allow us to draw some general conclusions about the relative behavior of the four nucleobases on Au(111) and about the performance of density functional theory for these systems.

- DFT calculations that include the long-term vdW interaction reveal that a horizontal adsorption geometry is always preferred over a vertical mode, practically degenerate in the case of cytosine.[40] In fact, the full circles in Figure 3 lie always at lower/same energies than the full squares. This is a genuine result of our approach, while the relative energetics is erroneously described if the long-range vdW interaction is not included.[33] We remark that experimental results on monolayers indicate that DNA bases are horizontal relative to the substrate:[41,44,45,47] thus, our results are in line with observations.
- The adsorption energy from vdW−DF calculations is systematically larger than that from PBE calculations, by three to six times. This was already observed for horizontal C@Au(111) and is confirmed here over a much larger sample. There is one single exception, the case of vertical cytosine, which is separately discussed later.
- The molecule−surface distance (Table 1) is similar in horizontal and vertical adsorption configurations for the same base. It is also similar for the different bases. It is usually larger from PBE than from vdW−DF calculations, except for structures ${}_{\nu}\mathrm{C@Au(111)}^{t+N3t}$ and ${}_{\nu}\mathrm{A@Au(111)}^{N3t}$. vdW−DF results on adsorption distances are in fair agreement with a variety of results on aromatic systems and heterocycles,[66,67] while PBE results fail.
- The values of the interaction energy and the analysis of the electronic structure suggest a moderately strong molecule/substrate coupling, beyond the pure van der Waals regime, that would hint to a smaller distance between the molecule and the surface. This is, in fact, in line with the already known overestimation of equilibrium distances characteristic of the vdW−DF functional.[51,57,68,69]
- The vdW interaction has impact not only on the adsorption energies and molecule−surface distances but also affects the relative orientation of the adsorbate to the substrate. This is particularly true for cytosine[40] and guanine in horizontal configurations, in which the molecular plane is tilted with respect to the surface plane, while this is not the case in PBE calculations. The importance of van der Waals terms in DFT calculations of DNA bases on Cu(111) was recently analyzed, with qualitatively similar conclusions.[70]
- O atoms are the most reactive centers in the DNA bases, followed by N atoms. Cytosine, guanine, and thymine preferentially interact with the Au(111) surface through O atoms (O2, O6, and O2+O4, respectively), and also the N atoms that are not saturated by H atoms take part in the binding mode.[40] Adenine can interact with the Au(111) surface through N1, N3, and N6. O and N atoms overall prefer top adsorption sites, where they are able to form bonding orbitals with the gold *d* bands (see subsection 3.2). As a result of their favored position outside the aromatic ring, O atoms are the ones that stay closer to the surface.
- The adsorption energy of the horizontal configurations is fairly independent of the adsorption site: 17, 20, 20, and 23 kcal/mol for T, C, A, and G, respectively (Table 1). In fact, although O and N prefer top adsorption sites, the spread of adsorption energy among the different sampled geometries for a particular base and a particular orientation is rather small (1.5 kcal/mol), indicating a rather flat energy profile for lateral mobility, in line with mobility data from molecular dynamics simulations.[71] In vertical configurations there is more spreading, especially when N atoms are involved in the adsorption mode.
- Guanine is the DNA base that interacts most strongly with the surface, while thymine interacts most weakly: the order of adsorption strength is $T < C \sim A < G$. This result is in agreement with the trend from experimental results on monolayers,[48] while in PBE calculations the desorption order is $A < T < C < G$.

A common behavior among the different nucleobases can also be traced by comparing the adsorption geometries of each base on the surface and in the gas phase (Tables S1−S5 in Supporting Information). First of all, the distortion of the adsorbed molecule relative to the gas-phase molecule are more marked in vertical configurations than in horizontal configurations. In all the adsorption systems treated in this work the

C−O bond length is elongated when the molecule is close to the surface. Guanine is the molecule that undergoes the largest changes in bond lengths, while the opposite extreme is thymine. In all the bases, bond lengths and angles change less than 1.5% upon adsorption. These structural changes are comparable in PBE and vdW−DF calculations. In the remainder of this subsection, we discuss specifically each base.

Cytosine. For C@Au(111) in horizontal configurations, we refer the reader elsewhere.[40] We only summarize here the salient factors: (1) the preferred adsorption mode is at the top site, though the energy difference for the other two possible choices is tiny; (2) the molecule is tilted by 76° with respect to the vertical axis, namely 14° relative to the surface plane.

Among the viable vertical configurations, cytosine likes to approach the substrate with both the O2 and N3 atoms. In fact, as already noted, nitrogen atoms that are not saturated by H atoms can interact with the Au(111) surface if they are close enough to it. This behavior was recently described for other systems, such as imidazole on Au(111).[29]

The ${}_{v}C@Au(111)^{t+N3t}$ configuration is almost isoenergetic with the horizontal ones, within 0.4 kcal/mol; instead, the other bases adopt horizontal configurations more favorably (by 4.7, 6.2, and 2.3 kcal/mol for G, T, and A, respectively). In this configuration, both the O2 and N3 atoms are located above top sites of the Au(111) triangular lattice. Comparing the PBE and vdW−DF results for the adsorption energy of ${}_{v}C@Au(111)^{t+N3t}$, we argue that the interaction is mainly short-range. In fact, the small energy difference of 3.7 kcal/mol indicates that PBE performs rather well, which is not true in situations where vdW effects are strong (as in the other configurations, for which the difference in formation energy between vdW−DF and PBE calculations is larger). This good performance of the PBE functional is peculiar of configurations with a concomitant binding of O and N atoms, as we also describe for *G@Au*(111). Despite such a similarity between the PBE and vdW−DF adsorption energy values, the computed molecule−surface distances at the two different levels of theory are quite dissimilar. Normally vdW−DF distances are smaller than PBE distances, although they are still overestimated relative to experimental data;[51,57,68,69] yet, the ${}_{v}C@Au(111)^{t+N3t}$ structure is an exception to this trend, with a PBE distance of 2.2 Å, much smaller than the vdW−DF value of 2.6 Å. We are confident that the correct description of the geometry is closer to the vdW−DF result than to the PBE result.

Both the energetics and the electronic structure of the peculiar ${}_{v}C@Au(111)^{t+N3t}$ configuration are very similar to those of the other cytosine adsorption geometries. This suggests for all the sampled cytosine interfaces the occurrence of the same kind of short-range interaction between the adsorbate and the surface. The inclusion of the short-range vdW coupling in the DFT functional is crucial to attain a correct description: in fact, the vdW−DF coupling allows the molecule to get close enough to the surface in order to feel the correct surface field and establish the bonding between Au and O/N atoms. Therefore, both short-range and long-range effects are important for the binding mode of cytosine on Au(111).

For a deeper inspection of the relative energetics between C@Au(111) structures, we performed some test calculations starting from intermediate configurations between horizontal and vertical, with both O and N atoms close to the surface and the molecule tilted at different angles. These tests indicate that the molecule favors a horizontal orientation. Thus, although horizontal and vertical geometries have similar adsorption energies and can coexist, the energy profile is such that the horizontal adsorption mode is selected more frequently, or on a larger portion of the substrate.

Guanine. For what concerns horizontal configurations, guanine on Au(111) behaves very similarly to cytosine. The three adsorption sites available to the O6 atoms are practically isoenergetic, within 0.3 kcal/mol. The molecule is not exactly parallel to the surface plane. The O−Au vertical distance is 3.0 Å at the top site.

We calculated five vertical configurations, with the O atom, a N atom, or atoms of both species oriented toward the surface. The ${}_{v}G@Au(111)^{t+N7t}$ structure has the lowest formation energy among the vertical guanine adsorption geometries: it is almost degenerate with ${}_{v}G@Au(111)^{b+N7t}$ and has a formation energy difference of 2÷3 kcal/mol relative to the other ${}_{v}G@Au(111)$ structures (Table 1). The lowest energy vertical structure for guanine has both the O2 and N7 atoms above top sites of the substrate lattice and interacting with Au; this situation is comparable to that of the ${}_{v}C@Au(111)^{t+N3t}$ configuration discussed above.

As for cytosine, also for guanine the preferred (by 5÷8 kcal/mol) adsorption orientation is horizontal, with a tilt angle between 3 and 7 degrees relative to the surface plane.

Thymine. Thymine is the base that has the weaker interaction with the Au(111) surface, despite the presence of two O atoms that are potential strong binders to Au: the horizontal configurations have adsorption energies between 16.9 and 17.2 kcal/mol and the vertical configurations between 7.5 and 11.0 kcal/mol. The CH_3 group in our optimized structures is oriented with one H atom on the plane of the molecule, one above and one below (Figure 1). Calculations were done to check other possible orientations of the CH_3 group that would imply a minor steric hindrance and the possibility for thymine to get closer to the surface. Independently of the starting orientation of the CH_3 group, this rotates back to a situation with high steric hindrance. This is the origin of the comparatively weak interaction of thymine with the Au(111) surface.

The deepest energy minumum is found for the ${}_{h}T@Au(111)^{t+f}$ horizontal configuration with the O2 atom at a top site and the O4 atom at a fcc site. All the other computed horizontal thymine structure, including ${}_{h}T@Au(111)^{f+t}$ in which O2 and O4 are simply exchanged at fcc and top sites, are almost isoenergetic, within 0.3 kcal/mol.

In all the horizontal ${}_{h}T@Au(111)$ configurations, thymine is slightly inclined relative to the surface plane, by 2÷6 degrees. The O2 and O4 atoms of thymine remain quite far from the surface with respect to the O2 atom of cytosine, consistently with the smaller energy gain upon adsorption.

The vertical T@Au(111) configurations are higher in energy by at least 6.2 kcal/mol than the preferred horizontal structure. The lowest-energy vertical configuration is with both the O2 and O4 atoms close to the surface (at either top+bridge or fcc +bridge sites), followed by that with the O2−C bond perpendicular to the (111) plane.

Adenine. Adenine is the only DNA base without an O atom, so the choice of strucutures was based on locating the N3 and N7 atoms above lattice sites.

Similarly to the other bases, the difference in adsorpton energies between different sites is quite small, practically vanishing for the horizontal configurations and within 2.5 kcal/mol for the vertical configurations.

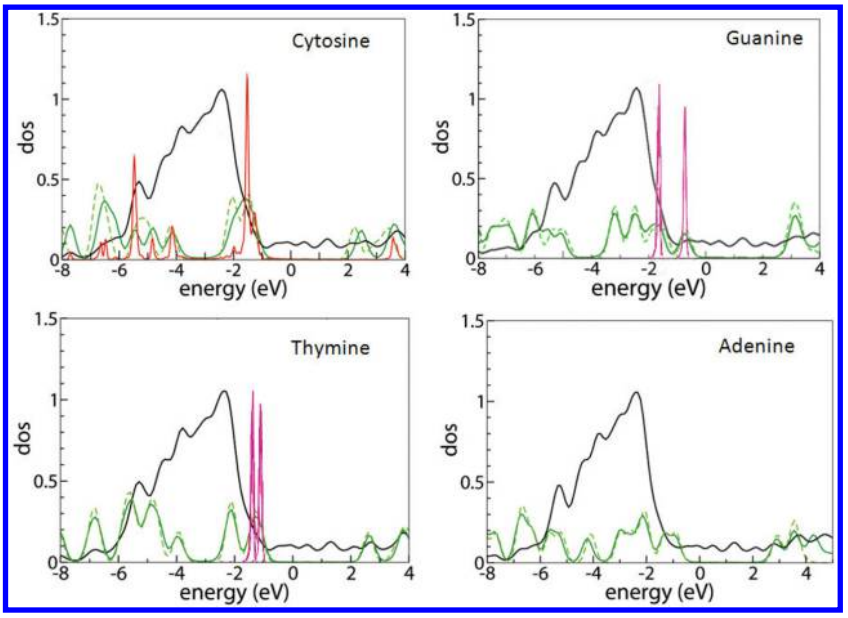

Figure 4. Density of states for the four bases adsorbed horizontally on the Au(111) surface, computed with the vdW−DF functional. In each plot, the Fermi level of the system is set at the origin of the energy scale and the deepest energy level, which is associated to the same orbital in the gas-phase molecule and in the adsorbed molecule, is used for alignment of the various curves. The green dashed (solid) line is the DOS of the gas-phase molecule (total DOS of the interface projected onto the molecule). The black line represents the sum of the projections of the total base/Au DOS on the adsorbate and on the outermost substrate layer. The red line in the top left panel is the projection of the cytosine/Au(111) DOS on the O2 atom. The black, red, and solid green projected DOS curves are computed by projecting the total DOS onto atomic orbitals and then summing over all the projections that constitute the subsystems of interest. The magenta line in the top right and bottom left panels is the sum of the projections of the total DOS onto the HOMO and HOMO − 1 molecular states of the gas-phase guanine and thymine.

Even in the absence of O atoms, adenine adheres significantly to the Au(111) surface. The adsorption energy of the horizontal structures is comparable to that of the horizontal $_h$C@Au(111) structures, even slightly higher. Among the sampled vertical configurations, adenine prefers an orientation with the NH_2 group opposite to the surface, so that the N3 atom, which is particularly reactive, can get close to a top site.

We end this section with an interesting analogy to another technologically relevant system, namely DNA bases on a graphene layer.[61,62] Stacked configurations of DNA bases on graphene can occur during translocation of a single-stranded DNA molecule through a nanopore and may affect the conductance of the graphene sheet in a way that can be exploited for fast DNA sequencing.[72] A graphene sheet is a metal, as the Au(111) surface is, which is the source of the analogy; note, however, that the metallic nature has a different physico−chemical nature in the two substrates. The structural analysis presented above basically concludes that DNA bases adsorb on Au(111) in a horizontal orientation, with binding strength in the order G (23 kcal/mol) > C ∼ A (20 kcal/mol) > T (17 kcal/mol), with the values of the interaction energy dominated by van der Waals effects. These features are almost exactly matched in the interfaces between DNA bases and graphene, where the horizontal adsorption orientation is also preferred and the binding energies are also around 20 kcal/mol. The only slight difference between base/Au(111) and base/graphene interfaces is the order of adsorption strength. In fact, in base/graphene interfaces, it was found that the order is G (22 kcal/mol) > A (20 kcal/mol) > T (19 kcal/mol) > C (17 kcal/mol).[61] The honeycomb lattice of graphene systematically prefers adsorption configurations in which the reactive atom in the base is above the center of a hexagon. Instead, we find that the (111) lattice of the gold surface accommodates the O atom of G and C at a top site: while for G the binding energy at different Au(111) sites is the same (Table 1), there is an energy gain of 2 kcal/mol for C from the fcc to the top site. This explains the larger stability of C at the Au(111) surface than at the graphene sheets and accounts for the different stability order. Note, however, that the energy differences are within 1−2 kcal/mol, which is at the limit of resolution of this type of calculations. The analogy traced here suggests a possible general behavior for the binding energy of DNA bases on metal surfaces and opens the way to a variety of possible applications of DNA/crystal interfaces.

3.2. Electronic Structure. We show in Figure 4 the plots of the electronic density of states (DOS) for the most favorable structures $_h$C@Au(111)^t, $_h$G@Au(111)^t, $_h$T@Au(111)$^{t+f}$, and $_h$A@Au(111)^b. The color code is explained in the figure caption. We note that the DOS of thymine and adenine is not significantly affected by the interaction with gold (similarity of the green solid and dashed lines), while in cytosine and guanine, we observe a redistribution of the DOS peaks for the adsorbed molecules in the energy range of the Au *d* bands. This finding is in line with the energetic and structural results. In fact, thymine and adenine exhibit negligible relaxation of the bond lengths and angles upon adsorption on Au(111) relative to the gas phase, and thymine is the DNA base that has the smallest adsorbate−substrate interaction energy. Cytosine and guanine, instead, undergo larger atomic distortions upon adsorption and gain more energy. These effects are not biased by the use of the vdW−DF functional (see Supporting Information, Figure S5).

The projections of the total DOS onto molecular states (magenta lines in Figure 4) indicate that the HOMO lies above the Au *d* bands for all the computed interfaces, even if shown

dx.doi.org/10.1021/ct4002416 | J. Chem. Theory Comput. 2013, 9, 4552−4561

only for guanine and thymine. The same is true for the HOMO − 1, with the exception of the G@Au(111) interface that we address separately below. Hybridization occurs between the HOMO and HOMO − 1 of cytosine, thymine and adenine and *d* orbitals of gold; however, the shape of such molecular orbitals is not affected by the interaction and no bonding orbitals are formed between the base and gold.

We note that, interestingly, DOS molecular features are present in energy ranges where the Au DOS is also non-negligible. We inspected such energy ranges to search for hybrid molecule−Au orbitals that would reveal some electronic coupling, encouraged by the findings in similar or related systems.[29,40,55] The systematic analysis of all the single-particle electron wave functions reveals the formation of bonding orbitals between the adsorbate and the substrate in the energy range of Au *d* bands. This is true for the four bases, for both horizontal and vertical configurations, despite the fact that the DOS of T@Au(111) and A@Au(111) interfaces does not show appreciable differences relative to the DOS of the respective gas-phase molecule. We find that the formation of bonding orbitals requires the participation of a molecular orbital with a charge component on the most reactive atoms O and N. Bonding orbitals (Figure 5) are accomplished in the energy

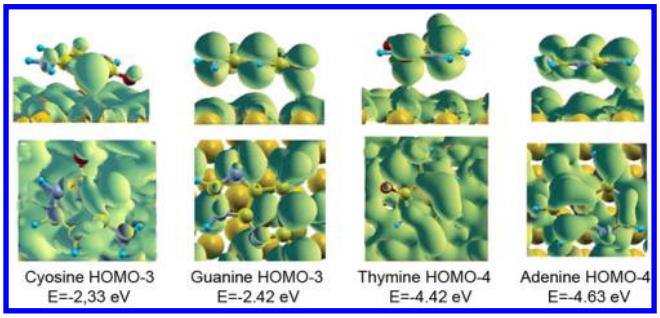

Figure 5. Isosurface plots of representative bonding orbitals formed by cytosine, guanine, thymine, and adenine with gold. These representative examples pertain to the lowest-energy interfaces (gray cells in Table 1).

range between −6.0 and −1.5 eV, namely in the domain of the Au *d* bands (Figure 4). For all the computed interfaces, the HOMO − 3 and HOMO − 4 are mostly responsible for the formation of bonding orbitals with Au. In the case of G@Au(111), also, the HOMO−1 of guanine forms bonding orbitals with *d* orbitals of Au, because of the relative energy of this orbital in the gas phase and the Au bands (Figure 4, top right panel).

The mechanism for electronic hybridization that we find in these systems is different from that characteristic of chemisorption systems.[55] The Newns−Anderson model for atomic and molecular chemisorption on transition metal surfaces predicts that the interaction between a localized atomic or molecular orbital and the narrow *d* band of the metal produces hybrid orbitals of both bonding and antibonding type. In the case of molecular chemisorption, the HOMO of the molecule is responsible for this mechanism.[55] The metal−HOMO bonding orbitals give a peak in the DOS of the molecule/metal interface at the lower−energy edge of the metal *d* bands and the metal−HOMO antibonding orbitals give a peak in the DOS at the upper−energy edge of the metal *d* bands.[73] This mechanism is found, for example, in thiols chemisorbed on Au(111)[56] but also in the case of molecular adsorbates with O and N anchoring groups instead of S.[74] It was accurately discussed in the case of cysteine/Au(111).[55] In the case of DNA bases adsorbed on Au(111) that we treat in this article, we have an alternative situation. We reveal the formation of bonding orbitals, but the overall electronic hybridization mechanism does not comply with the Newns−Anderson picture. We do not detect any bonding−antibonding splitting of the HOMO. Nay, the HOMO is not responsible at all for bonding-like hybridization. The molecular orbitals that form hybrid molecule−metal bonding orbitals are actually those that in the gas-phase molecule have energies coincident with those of Au *d* orbitals; such molecular orbitals do not show bonding−antibonding splitting but only a slight shift with respect to the isolated components.

On the other hand, this adsorption mechanism is also different from that typical of purely aromatic molecules. For pentacene on Cu(100),[75] for instance, it was shown that the slight electronic hybridization between the molecule and the surface occurs via partial filling of the LUMO orbital. This is not accompanied by the formation of any bonding states between occupied molecular orbitals and metal *d* orbitals.

4. SUMMARY

In this paper, we have investigated by means of first-principles electronic structure calculations several interfaces formed by cytosine, guanine, thymine, and adenine with the Au(111) surface, with the objectives of interpreting the adsorbate−substrate interaction mechanism and developing a classical force field for related systems constituted of DNA oligomers on Au(111). We showed that vdW effects are main determinants to attain a correct description of the computed interfaces, both qualitatively and quantitatively. We gave insights into the adsorption mechanism of these heterocycles, which is different from that typical of homocycles[75] on one hand and of non-planar molecules (e.g., thiols)[55] on the other hand. These results are the basis for enabling classical molecular dynamics simulations of DNA on gold, through the generation of a tailored force field that will include adsorbate/substrate interaction and image charge effects.[26,27] In fact, the vdW−DF results on the structure and energetics of G, C, A, and T on Au(111) are being exploited to develop a first-generation AMBER-like force field to describe DNA/gold interfaces. The procedure is conceptually similar to what we recently did for protein/Au(111) interfaces,[26,29] but using data suitable to the adsorption of nucleobases rather than amino acids.

■ ASSOCIATED CONTENT

Supporting Information

Figures S1−S4 illustrate the most relevant optimized interfaces that appear in Table 1: Figure S1 for C@Au(111), Figure S2 for G@Au(111), Figure S3 for T@Au(111), Figure S4 for A@Au(111). Figure S5 illustrates the total DOS of $_h$G@Au(111)^t computed with the PBE and vdW−DF functionals. Tables S1−S5 report the changes in molecular bond lengths and bond angles when the molecule goes from the gas phase to the adsorbed phase, in selected most favorable configurations: Tables S1 and S2 for C@Au(111), Table S3 for G@Au(111), Table S4 for T@Au(111), Table S5 for A@Au(111). This material is available free of charge via the Internet at http://pubs.acs.org/.

AUTHOR INFORMATION

Corresponding Author

*E-mail: rosa.difelice@unimore.it.

Notes

The authors declare no competing financial interest.

ACKNOWLEDGMENTS

This work was funded by the European Commission through project "DNA-Nanodevices" (Contract No. FP6-029192), by the ESF through the COST Action MP0802, by the Italian Institute of Technology through project MOPROSURF and the Computational Platform, by Fondazione Cassa di Risparmio di Modena through Progetto Internazionalizzazione 2011. The ISCRA staff at CINECA (Bologna, Italy) is acknowledged for computational facilities and technical support. Fengzhu Sun and Remo Rohs are gratefully acknowledged for their crucial support of extended visits in Rohs laboratory at the University of Southern California in Los Angeles during the final stages of this work.

REFERENCES

(1) Miescher, F. *Medicinischchemische Untersuchungen* **1871**, *4*, 441−460.
(2) Dahm, R. *Am. Sci.* **2008**, *96*, 320−327.
(3) Watson, J. D.; Crick, F. H. *Nature* **1953**, *171*, 737−738.
(4) Porath, D.; Cuniberti, G.; Di Felice, R. *Top. Curr. Chem.* **2004**, *237*, 183−227.
(5) Endres, R. G.; Cox, D. L.; Singh, R. R. P. *Rev. Mod. Phys.* **2004**, *76*, 195−214.
(6) Mallajosyula, S. S.; Pati, S. K. *J. Phys. Chem. Lett.* **2010**, *1*, 1881−1894.
(7) Genereux, J. G.; Barton, J. K. *Chem. Rev.* **2010**, *110*, 1642−1662.
(8) Shapir, E.; Calzolari, A.; Cavazzoni, C.; Ryndyk, D.; Cuniberti, G.; Kotlyar, A. B.; Di Felice, R.; Porath, D. *Nat. Mater.* **2008**, *7*, 68−74.
(9) Shapir, E.; Sagiv, L.; Molotsky, T.; Kotlyar, A. B.; Di Felice, R.; Porath, D. *J. Phys. Chem. C* **2010**, *114*, 22079−22084.
(10) Lindsay, S. M.; Thundat, T.; Nagahara, L. A. *J. Microsc.* **1988**, *152*, 213−220.
(11) de Pablo, P. J.; Moreno-Herrero, F.; Colchero, J.; Gómez Herrero, J.; Herrero, P.; Baró, A. M.; Ordejón, P.; Soler, J. M.; Artacho, E. *Phys. Rev. Lett.* **2000**, *85*, 4992−4995.
(12) Kotlyar, A. B.; Borovok, N.; Molotsky, T.; Cohen, H.; Shapir, E.; Porath, D. *Adv. Mater.* **2005**, *17*, 1901−1905.
(13) Porath, D.; Bezryadin, A.; de Vries, S.; Dekker, C. *Nature* **2000**, *403*, 635−638.
(14) Cohen, H.; Nogues, C.; Naaman, R.; Porath, D. *Proc. Natl. Acad. Sci. U.S.A.* **2005**, *102*, 11589−11593.
(15) Boon, E. M.; Barton, J. K. *Curr. Opin. Struct. Biol.* **2002**, *12*, 320−329.
(16) Slinker, J. D.; Muren, N. B.; Gorodetsky, A. A.; Barton, J. K. *J. Am. Chem. Soc.* **2010**, *132*, 2769−2774.
(17) Varsano, D.; Garbesi, A.; Di Felice, R. *J. Phys. Chem. B* **2007**, *111*, 14012−14021.
(18) Migliore, A.; Corni, S.; Varsano, D.; Klein, M. L.; Di Felice, R. *J. Phys. Chem. B* **2009**, *113*, 9402−9415.
(19) Woiczikowski, P.; Kubar, T.; Gutierrez, R.; Caetano, R.; Cuniberti, G.; Elstner, M. *J. Chem. Phys.* **2009**, *130*, 215104/1−14.
(20) Woiczikowski, P.; Kubar, T.; Gutierrez, R.; Cuniberti, G.; Elstner, M. *J. Chem. Phys.* **2010**, *133*, 035103/1−12.
(21) Daggett, V.; Levitt, M. *J. Mol. Biol.* **1993**, *232*, 600−618.
(22) Tirado−Rives, J.; Orozco, M.; Jorgensen, W. L. *Biochem.* **1997**, *36*, 7313−7329.
(23) Toofanny, R. D.; Daggett, V. *WIREs Comput. Mol. Sci.* **2012**, *2*, 405−423.
(24) Allen, M. P.; Tildesley, D. J. *Computer Simulation of Liquids*; Oxford University Press: Oxford, 1987; pp 1−385.
(25) van Gusteren, W. F.; Berendsen, H. J. C. *Angew. Chem., Int. Ed.* **1990**, *29*, 992−1023.
(26) Iori, F.; Di Felice, R.; Molinari, E.; Corni, S. *J. Comput. Chem.* **2009**, *30*, 1465−1476.
(27) Wright, L. B.; Rodger, P. M.; Corni, S.; Walsh, T. *J. Chem. Theor. Comput.* **2013**, *9*, 1616−1630.
(28) Di Felice, R.; Corni, S. *J. Phys. Chem. Lett.* **2011**, *2*, 1510−1519.
(29) Iori, F.; Corni, S.; Di Felice, R. *J. Phys. Chem. C* **2008**, *112*, 13540−13545.
(30) Wong, K.-Y.; Pettitt, B. M. *Teor. Chim. Acta* **2001**, *106*, 233−235.
(31) Zwolak, M.; Di Ventra, M. *Rev. Mod. Phys.* **2008**, *80*, 141−165.
(32) Hughes, G. A. *Nanomedicine* **2005**, *1*, 22−30.
(33) Piana, S.; Billic, A. *J. Phys. Chem. B* **2006**, *110*, 23467−23471.
(34) Otero, R.; Lukas, M.; Kelly, R. E. A.; Xu, W.; Laegsgaard, E.; Stensgaard, I.; Kantorovich, L. N.; Besenbacher, F. *Science* **2008**, *319*, 312−315.
(35) Ortmann, F.; Schmidt, W. G.; Bechstedt, F. *Phys. Rev. Lett.* **2005**, *95*, 186101/1−4.
(36) Sowerby, S. J.; Stockwell, P. A.; Heckl, W. M.; Petersen, G. B. *Origins Life Evol. Biospheres* **2000**, *30*, 81−99.
(37) Seino, K.; Schmidt, W. G.; Preuss, M.; Bechstedt, F. *J. Phys. Chem. B* **2003**, *107*, 5031−5035.
(38) Kilina, S.; Tretiak, S.; Yarotski, D. A.; Zhu, J.-X.; Modine, N.; Taylor, A.; Balatsky, A. V. *J. Phys. Chem. C* **2007**, *111*, 14541−14551.
(39) Mignon, P.; Ugliengo, P.; Sodupe, M. *J. Phys. Chem. C* **2009**, *113*, 13741−13749.
(40) Rosa, M.; Corni, S.; Di Felice, R. *J. Phys. Chem. C* **2012**, *116*, 21366−21373.
(41) Kelly, R. E. A.; Xu, W.; Lukas, M.; Otero, R.; Mura, M.; Lee, Y-J.; Laegsgaard, E.; Stensgaard, I.; Kantorovich, L. N.; Besenbacher, F. *Small* **2008**, *4*, 1494−1500.
(42) Lukas, M.; Kelly, R. E. A.; Kantorovich, L. N; Otero, R.; Xu, W.; Laegsgaard, E.; Stensgaard, I.; Kantorovich, L. N.; Besenbacher, F. *J. Chem. Phys.* **2009**, *130*, 024705/1−9.
(43) Xu, W.; Kelly, R. E. A.; Henkjan, G.; Laegsgaard, E.; Stensgaard, I.; Kantorovich, L. N.; Besenbacher, F. *Small* **2009**, *5*, 1952−1956.
(44) Xu, W.; Kelly, R. E. A.; Otero, R.; Schöck, M.; Laegsgaard, E.; Stensgaard, I.; Kantorovich, L. N.; Besenbacher, F. *Small* **2007**, *3*, 2011−2014.
(45) Kelly, R. E. A.; Lukas, M.; Kantorovich, L. N.; Otero, R.; Xu, W.; Mura, M.; Laegsgaard, E.; Stensgaard, I.; Besenbacher, F. *J. Chem. Phys.* **2008**, *129*, 187707.
(46) Otero, R.; Lukas, W. X. M.; Kelly, R. E. A.; Xu, W.; Laegsgaard, E.; Stensgaard, I.; Kantorovich, L. N.; Besenbacher, F. *Science* **2008**, *319*, 312−315.
(47) Kelly, R. E. A.; Lukas, M.; Kantorovich, L. N.; Otero, R.; Xu, W.; Mura, M.; Laegsgaard, E.; Stensgaard, I.; Besenbacher, F. *J. Chem. Phys.* **2008**, *129*, 184707/1−13.
(48) Ostblom, M.; Liedberg, B.; Demers, L. M.; Mirkin, C. A. *J. Phys. Chem. B* **2005**, *109*, 15150−15160.
(49) Giannozzi, P.; Baroni, S.; Bonini, N.; Calandra, M.; Car, R.; Cavazzoni, C.; Ceresoli, D.; Chiarotti, G. L.; Cococcioni, M.; Dabo, I.; Dal Corso, A.; de Gironcoli, S.; Fabris, S.; Fratesi, G.; Gebauer, R.; Gerstmann, U.; Gougoussis, C.; Kokalj, A.; Lazzeri, M.; Martin-Samos, L.; Marzari, N.; Mauri, F.; Mazzarello, R.; Paolini, S.; Pasquarello, A.; Paulatto, L.; Sbraccia, C.; Scandolo, S.; Sclauzero, G.; Seitsonen, A. P.; Smogunov, A.; Umari, P.; Wentzcovitch, R. *J. Phys.: Condens. Matter* **2009**, *21*, 395502/1−19.
(50) Perdew, J. P.; Burke, K.; Ernzerhof, M. *Phys. Rev. Lett.* **1996**, *77*, 3865−3868.
(51) Dion, M.; Rydberg, H.; Schroder, E.; Langreth, D. C.; Lundqvist, B. I. *Phys. Rev. Lett.* **2004**, *92*, 246401/1−4.
(52) Vanderbilt, D. *Phys. Rev. B* **1990**, *41*, R7892−R7895.
(53) Akinaga, Y.; Nakajima, T.; Hirao, K. *J. Chem. Phys.* **2001**, *114*, 8555−8564.
(54) Fernandez, E. M.; Soler, J. M.; Balbas, L. C. *Phys. Rev. B* **2008**, *73*, 235433/1−8.

(55) Di Felice, R.; Selloni, A.; Molinari, E. *J. Phys. Chem. B* **2003**, *107*, 1151−1156.
(56) Vargas, M. C.; Giannozzi, P.; Selloni, A.; Scoles, G. *J. Phys. Chem. B* **2001**, *105*, 9509−9513.
(57) Thonhauser, T.; Cooper, V. R.; Li, S.; Puzder, A.; Hyldgaard, P.; Langreth, D. C. *Phys. Rev. B* **2007**, *76*, 125112/1−11.
(58) Langreth, D. C.; Dion, M.; Rydberg, H.; Schroder, E.; Hyldgaard, P.; Lundqvist, B. I. *Int. J. Quantum Chem.* **2005**, *101*, 599−610.
(59) Tkatchenko, A.; Romaner, L.; Hofmann, O. T.; Zojer, E.; Ambrosch-Draxl, C.; Scheffler, M. *MRS Bull.* **2010**, *35*, 435−442.
(60) Vanin, M.; Mortensen, J. J.; Kelkkanen, A. K.; Garcia-Lastra, J. M.; Thygesen, K. S.; Jacobsen, K. W. *Phys. Rev. B* **2010**, *81*, 081408/1−4.
(61) Cho, Y.; Min, S. K.; Yu, J.; Kim, W. Y.; Tkachenko, A.; Kim, K. S. *J. Chem. Theor. Comput.* **2013**, *9*, 2090−2096.
(62) Antony, J.; Grimme, S. *Phys. Chem. Chem. Phys.* **2008**, *10*, 2722−2729.
(63) Mura, M.; Gulans, A.; Thonhauser, T.; Kantorovich, L. *Phys. Chem. Chem. Phys.* **2010**, *12*, 4759−4767.
(64) Atodiresei, N.; Caciuc, V.; Lazić, P.; Blügel, S. *Phys. Rev. Lett.* **2009**, *102*, 136809/1−4.
(65) Johnston, K.; Harmandaris, V. *J. Chem. Phys. C* **2011**, *115*, 14707−14717.
(66) Tautz, F. S. *Prog. Surf. Sci.* **2007**, *82*, 479−520.
(67) Henze, S. K. M.; Bauer, O.; Lee, T-L.; Sokolowski, M.; Tautz, F. S. *Surf. Sci.* **2007**, *601*, 1566−1573.
(68) Lee, K.; Murray, E. D.; Kong, L.; Lundqvist, B. I.; Langreth, D. C. *Phys. Rev. B* **2010**, *82*, 081101(R)/1−4.
(69) Puzder, A.; Dion, M.; Langreth, D. C. *J. Chem. Phys.* **2006**, *124*, 164105/1−8.
(70) Bogdan, D.; Morari, C. *J. Phys. Chem. A* **2013**, *117*, 4669−4678.
(71) Rapino, S.; Zerbetto, F. *Langmuir* **2005**, *21*, 2512−2518.
(72) Min, S. K.; Kim, W. Y.; Cho, Y.; Kim, K. S. *Nature Nanotechnol.* **2011**, *6*, 162−165.
(73) Hammer, B.; Nørskov, J. K. *In Theory of Adorption and Surface Reactions, in Chemisorption and Reactivity of Supported Clusters and Thin Films*; Lambert, R. M., Pacchioni, G., Eds.; Kluwer Academic Publishers: The Netherlands, 1997; pp 285−351.
(74) Gori, P.; Contini, G.; Prosperi, T.; Catone, D.; Turchini, S.; Zema, N.; Palma, A. *J. Phys. Chem. B* **2008**, *112*, 3963−3970.
(75) Ferretti, A.; Calzolari, A.; Di Felice, R.; Ruini, A.; Molinari, E.; Baldacchini, C.; Betti, M. G. *Phys. Rev. Lett.* **2007**, *99*, 046802/1−4.